JOURNAL OF THE KOREAN ASTRONOMICAL SOCIETY
38: 121 ~ 124, 2005

NUCLEAR SPIRALS IN NEARBY GALAXIES

HONG BAE ANN
Division of Science Education, Pusan National University, Busan, 609-735, Korea
E-mail: hbann@pusan.ac.kr
(Received February 1, 2005; Accepted March 15, 2005)

ABSTRACT

High resolution images of the nuclear regions of nearby galaxies show that nuclear spirals are preponderant in normal galaxies as well as in active galaxies. These nuclear spirals, especially the grand-design nuclear spirals are found to be formed by the gas flow driven by the bar. Hydrodynamical simulations exploring a wide range of parameter space show that the morphology of nuclear spirals depends not only on the inner dynamics but on the global dynamics resulting from the global mass distribution of galaxies. Thus, the nuclear morphology can be a diagnostic tool for the inner dynamics of galaxies when the global mass distribution is taken into account.

Key words : galaxies: evolution — galaxies:nuclei — galaxies: structure — method — numerical

I. INTRODUCTION

High resolution images of nuclear regions of nearby galaxies show that more than half of nearby galaxies have nuclear spirals in the central kiloparsecs of galaxies. They have a variety of morphology, including chaotic spirals and grand-design ones (Martini *et al.* 2003). There have been a few mechanisms proposed for the formation of the nuclear spirals in nearby galaxies: acoustic instability for flocculent nuclear spirals (Elmegreen *et al.* 1998; Montenegro, Yuan & Elmegreen 1999), gas density waves (Englmaier & Shlosman 2000) and hydrodynamic shocks (Marciewjeski *et al.* 2002) for grand-design nuclear spirals. Recently, Ann & Thakur (2005) proposed that nuclear spirals are formed by the hydrodynamic instability but gas density waves do roles to maintain them in the late phase of evolution.

As shown by Ann & Lee (2004), the openness of the grand-design nuclear spiral arms depends on the central mass concentration and the sound speed in the gas. However, owing to the correlation between them (Englmaier & Shlosman 2000), the morphology of a grand-design nuclear spirals can be a diagnostics for the central mass concentration which is mainly determined by the mass of an SMBH (Ann & Lee 2004). Here we present the results of smoothed particle hydrodynamics (SPH) simulations exploring a wide range of parameter space that extend the work of Ann & Lee (2004) to show the detailed dependence of the nuclear morphology on the mass model and the sound speed in the gas.

Proceedings of *the 6th East Asian Meeting of Astronomy*, held at Seoul National University, Korea, from October 18-22, 2004.

II. SIMULATIONS

(a) Numerical Methods

The present simulations are two-dimensional ones based on Fux(1999)'s SPH code with the assumption of an isothermal equation of state for the gas. We investigated the effect of gas sound speeds (c_s) on the evolution of the gaseous disks by varying c_s between 5 km/s to 35 km/s. We assumed external potentials for the halo, bulge, disk, and bar, together with a point mass potential for the SMBHs. The potentials are fixed in the frame co-rotating with the bar. We used the same potentials as those of Ann & Lee (2004) and Ann & Thakur (2005). The self-gravity of gas was included.

(b) Mass Models

We assumed four mass models in our simulations which differ in the mass of the model galaxy (M_G) and the disk-to-bulge ratio ($\frac{D}{B}$). We adopted $M_G \approx 2.5 \times 10^{11}\,\mathrm{M}_\odot$ and $M_G \approx 4 \times 10^{10}\,\mathrm{M}_\odot$ for the masses of massive models and less massive models, respectively. We assumed $\frac{D}{B} = 2$ for early type galaxies and $\frac{D}{B} = 5$ for late type ones. The massive mass models are employed to reproduce the rotation curves of massive galaxies whose maximum rotational velocity is ~ 300 km/s, while the less massive mass models are used to reproduce the rotation curves of which the maximum velocity is ~ 150 km/s. Since the dynamics of the nuclear regions is mostly governed by the mass of SMBHs (M_{bh}), we varied M_{bh} from 0 to 1 % of the total visible mass of model galaxies.

We adopted moderately strong bars whose axial ratio and fractional mass are fixed as $\frac{a}{b} = 3$ and $\frac{M_{bar}}{M_G} = 0.2$, respectively. The semi-major axis length of bar is assumed as 6 kpc for massive models and 3 kpc for less massive models. The scale lengths of halo, bulge and disk are selected to reproduce the rotation curves.

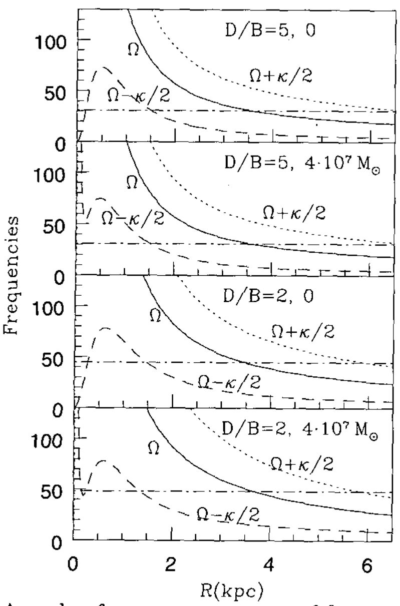

Fig. 1.— Angular frenquency curves of four model galaxies. The models differ in $\frac{D}{B}$ and M_{bh} which are given in the upper right part of each panel. The horizontal dot-dashed lines represent the pattern speeds of the bars.

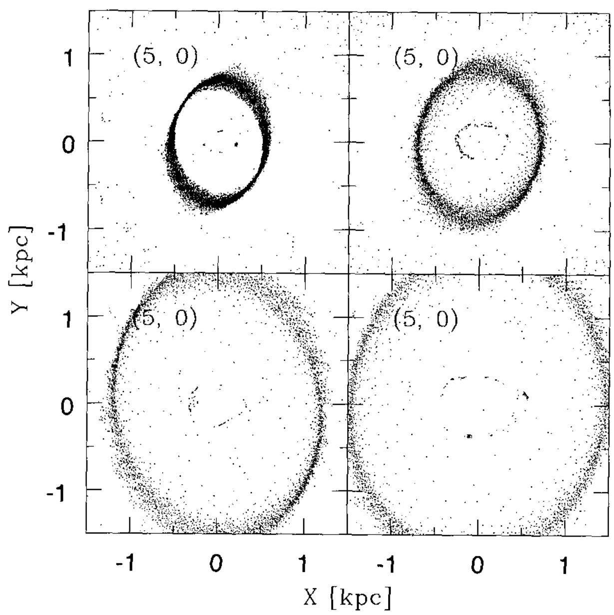

Fig. 2.— Snapshots of the central kiloparsecs of the gaseous disks at the evolution time of $\sim$ 7.2 bar rotations. Top panels represent less massive models while bottom panels show massive models. The Models in the left column have $\frac{D}{B} = 5$ and those in the right column have $\frac{D}{B} = 2$. The pair of numbers in the upper left corner of each panel represents c_s (km/s) and M_{bh} ($\times 10^7$ M$_\odot$), respectively. Here we assumed $c_s = 5$ km/s and $M_{bh} = 0$.

scale length for early and late type galaxies, respectively. Bars end near the co-rotation radii: $R_{CR} \approx 1.2a$ where a is the semi-major axis length of bar. The angular frequency curves of less massive models are given in Fig. 1.

(c) Initial Set Up

We distributed 20000 SPH particles randomly within the radius of 5 kpc and 10 kpc, respectively, for less massive models and massive models to represent initial uniform gaseous disks. The initial inter-particle distance, defined by $\sqrt{m/4\pi\Sigma}$, is 20 pc. Here m and Σ are the mass of each gas particle and the surface density of the initial gas disk. We introduced bar component gradually to avoid an abrupt evolution of gas particles. The full strength of the bar component was achieved after a half bar revolution.

III. RESULTS

The nuclear features, such as nuclear rings and nuclear spirals, observed in nearby galaxies are well reproduced by the present simulations. Our simulations exploring a wide range of parameter space show that the evolution of gaseous disk depends not only on the mass models but on the hydrodynamical properties. Here we present some typical models to demonstrate the dependence of the nuclear morphology on the mass models and the sound speeds in the gas.

In Figs. 2–5, we present the snapshots of the central kiloparsecs of gaseous disks at $\sim$ 7.2 bar rotations. The numbers in the upper left corner of each panel represent the gas sound speed and the mass of the SMBH, respectively. In Figs 2–4, the top left and top right panels present the less massive late type models ($M_G = 4 \times 10^{10}$ M$_\odot$, $\frac{D}{B} = 5$) and early type models ($M_G = 4 \times 10^{11}$ M$_\odot$, $\frac{D}{B} = 2$), whereas the bottom left and bottom right panels display the massive late type models ($M_G = 2.3 \times 10^{11}$ M$_\odot$, $\frac{D}{B} = 5$) and early type models ($M_G = 2.5 \times 10^{11}$ M$_\odot$, $\frac{D}{B} = 2$). As shown in Figs. 2–4, the central kiloparsecs of cold gaseous disks ($c_s < 10$ km/s) lead to the development of ring-like structures, regardless of mass models, whereas the morphology of the central kiloparsecs of hot gaseous disks ($c_s \gtrsim 10$ km/s) depends on the mass models as well as the sound speeds in the gas. The nuclear morphology developed in the cold gaseous disks in Fig. 2 resembles nuclear rings observed in nearby galaxies.

The dependence of the evolution of the hot gaseous disks on mass models is demonstrated in Fig. 3 and Fig. 4 where we assumed $c_s = 15$ km/s. Fig. 3 shows the snapshots of the mass models that do not have an SMBH in the center, while Fig. 4 displays those that have an SMBH whose mass is $\sim 0.01 \times M_G$. They clearly show that the nuclear morphology of barred galaxies depends not only on the global dynamics of the host galaxies which is determined by M_G and $\frac{D}{B}$ but also on the mass of central SMBHs. As shown in the models that have no SMBH (Fig. 3), the nuclear features developed in the less massive models look some-

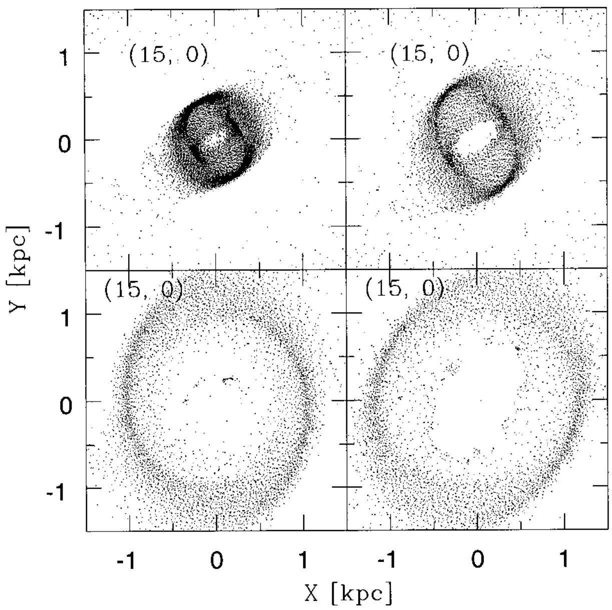

Fig. 3.— The same as Fig. 2 but we assumed c_s = 15 km/s and $M_{bh} = 0$.

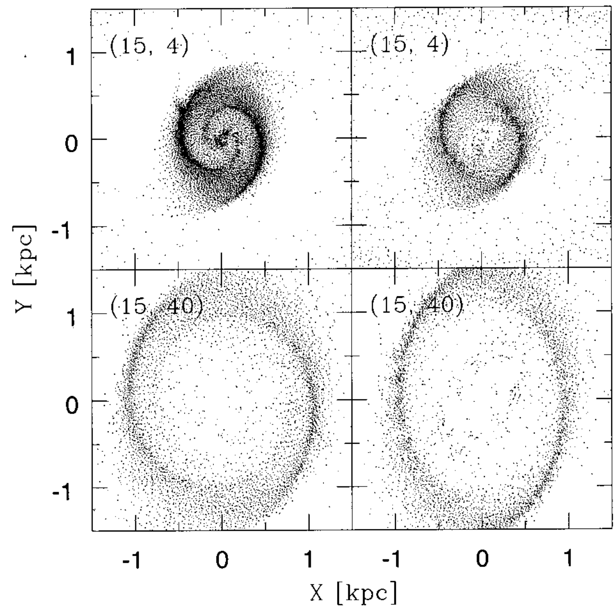

Fig. 4.— The same as Fig. 2 but we assumed c_s = 15 km/s and $M_{bh} = 4 \times 10^7 \, M_\odot$ and $40 \times 10^7 \, M_\odot$, for less massive galaxies and massive galaxies, respectively.

what similar to each other, but they differ much from those of the massive models. However, there seems to be some difference between the nuclear features of the massive models with $\frac{D}{B} = 2$ and that of the massive models with $\frac{D}{B} = 5$. The former shows somewhat short spiral arms with a large central empty zone, while the latter shows well developed spiral arms that wind more than $\frac{3}{2}\pi$ with a smaller empty zone. The spiral arm feature in the massive model with $\frac{D}{B} = 5$ in Fig. 3 resembles the ring-like nuclear spiral of NGC 4314 (Ann 2001; Benedict *et al.* 2002). In the late stage of evolution, the nuclear feature of less massive model with $\frac{D}{B} = 5$ evolves to round and thick nuclear ring while that of the less massive model with $\frac{D}{B} = 2$ evolves to an elongated ring or leading spiral. For massive models with $\frac{D}{B} = 5$, the ring-like spiral extends toward the center to make winding angle larger than 2π with a very elongated bar-like ring inside, whereas the nuclear feature of the massive model with $\frac{D}{B} = 2$ evolves to well defined leading spirals with a large empty zone inside. The formation of the empty zone is due to the negative torques from the bar at IILR.

When there is an SMBH that is massive enough to remove IILR, the dependence of the evolution of the nuclear features in the hot gaseous disks are much different from that of the models with no SMBH. In this case, the primary parameter that affects the nuclear morphology is not the galaxy mass but the global morphology represented by $\frac{D}{B}$. As shown in Fig. 4, the late type models show well developed nuclear spirals regardless of the mass of the model galaxy, while the early type models show elongated rings or very open spiral arms. However, the exact morphology of each mass model depends on the inner dynamics that is determined by the global mass distribution as well as the central mass concentration induced by SMBH. The ring-like spiral feature developed in the massive model of $\frac{D}{B} = 5$ in Fig. 4 is very similar to that in the same mass model but no SMBH (bottom left panel of Fig. 3). But, the late evolution of these two models is quite different. The ring-like spiral in Fig. 3 winds a little bit more and a very elongated ring forms inside the ring-like spiral, while the ring-like spiral in Fig. 4 extends toward the nucleus more and more, resulting in winding angles larger than 3π after 20 bar rotations.

The effect of the sound speed of gas on the nuclear morphology is demonstrated in Fig. 5. Here we present the snapshots of the central kiloparsecs of the gaseous disks of four massive models that assume $\frac{D}{B} = 5$ with varying sound speeds in the gas. As shown clearly in Fig. 5, the size of the nuclear features decreases as the gas sound speed increases. There is also a smooth change in the nuclear morphology in the sense that from the tightly wound features at low sound speeds to open features at high sound speeds. The nuclear ring developed in the models with c_s = 5 km/s is an extreme case of the tightly wound feature, while the open nulcear spiral in the models with c_s = 35 km/s is the opposite extreme case. It is also worth while to note that the innermost parts of the nuclear spirals reach close to the nucleus while the spiral arms become more opened. The correlation between the spiral arm morphology and the sound speeds in the gas can be understood in terms of the angular momentum evolution with the sound speeds in the gas (Ann & Thakur 2005).

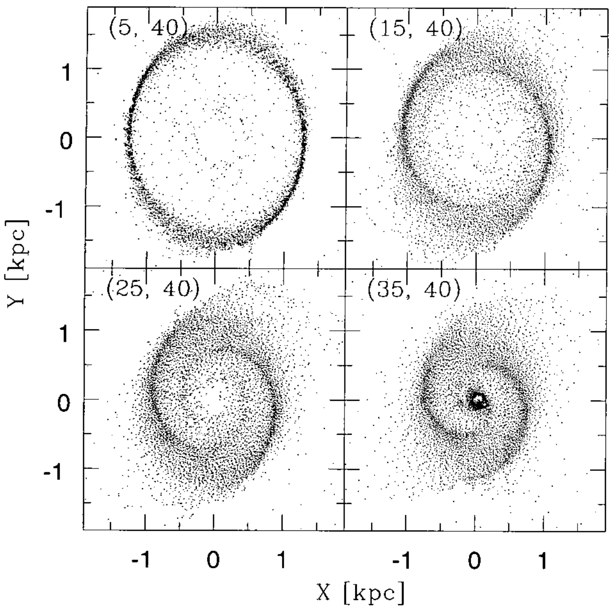

Fig. 5.— Snapshots of the central kiloparsecs of the gaseous disks of the massive models with $\frac{D}{B}$ = 5 at the evolution time of ~ 7.2 bar rotations. As shown in the pair of numbers in the upper left corner of each panel, we varied c_s from 5 km/s to 35 km/s but we fixed M_{bh} as $0.001 \times M_G$.

IV. DISCUSSION AND CONCLUSIONS

The correlation between the morphology of nuclear spirals characterized by the openness and winding angles, and the sound speeds in the gas (see Fig. 5) is frequently observed in the hydrodynamical simulations for the gas response to the imposed non-axisymmetric potentials (Englmaier & Gerhard 1997; Englmaier & Shlosman 2000; Ann & Lee 2004). However, the reason for the correlation is not well understood until recently. Ann & Thakur (2005) showed that the gas particles in highly turbulent motion, i.e., higher sound speeds, lose their angular momentum more easily than those in little turbulent motion, i.e., lower sound speeds. Thus, the nuclear spirals, formed by the gas particles which lost their angular momentum much, allow their innermost parts to reach close to the center, while those formed by the gas particles that lost their angular momentum little can not spiral in close to the center. Our extensive simulations show that the morphology of nuclear features developed in the central kiloparsecs depends not only on the inner dynamics but on the morphology of host galaxies. The dependence of the nuclear mophology on the inner dynamics that is mainly governed by the central mass concentration and the sound speeds in the gas is quite well known (Englmaier & Shlosman 2000; Ann & Lee 2004). But the dependence of the nuclear mophology on the global dynamics that determines the morphology of host galaxies is not much investigated yet. Since the global dynamics of a galaxy is determined by the mass distribution as a whole, it is important to consider the mass distribution far outside the nuclear regions even if we are interested only in the gas flows close to the nucleus.

It is found that the detailed morphology of nuclear spirals, characterized by the openness and winding angle, can be a diagnostics of the inner dynamics if we consider the morphology of the host galaxy together. The usefulness of nuclear spirals as diagnostic tools of the SMBHs has been reported by Ann & Lee (2004), but they did not mention about the effect of the global mass distribution on the morphology of the nuclear spirals since they considered less massive models ($M_G = 4 \times 10^{10}\,M_\odot$) only. We found that the correlation between the winding angles of the tightly wound nuclear spirals and the gas sound speed for late type galaxies and the anti-correlation between the openness of spiral arms and the mass of SMBH for early type galaxies (Ann & Lee 2004) hold for the coresponding massive models too. However, the plausible ranges of the gas sound speeds for the formation of tightly wound nuclear spirals, i.e., 15 ± 5 km/s for late type galaxies and 20 ± 5 km/s for early type galaxies (Ann & Lee 2004), are shifted to larger values, i.e., 25 ± 5 km/s for the massive late type galaxies and 30 ± 5 km/s for the massive early type galaxies, respectively.

ACKNOWLEDGEMENTS

This work was supported in part by the grant from ARCSEC. Most of the computations are conducted using the super computer facilities in KISTI.

REFERENCES

Ann, H. B., 2001, AJ, 121, 2515

Ann, H. B., & Lee, H. M., 2004, ApJ, 613L, 105

Ann, H. B., & Thakur, P., 2005, ApJ in press

Benedict, G. F., Howell, D. A., Jorgensen, I., Kenney, J. D. P., & Smith, B. J., 2002, AJ, 123, 1411

Elmegreen, B. G., Elmegreen, D. M., Brinks, E., Yuan, C., Kaufman, M., Klaric, M., Montenegro, L., Struck, C., & Thomasson, M., 1998, ApJ, 503, L119

Englmaier, P., & Gerhard, O. E., 1997, MNRAS, 287, 57

Englmaier, P., & Shlosman, R. S., 2000, ApJ, 528, 677

Fux, R.. 1999, A&A, 345,787

Long, K., & Murali, C., 1992, ApJ, 397, 44

Maciejewski, W., Teuben, P. J., Sparke, L. S., & Stone, J. M., 2002, MNRAS, 329, 502

Martini, P., Mulchaey, J. S., & Pogge, R. W., 2003, ApJ, 146, 353

Montenegro, L. E., Yuan, C., & Elmegreen, B. G., 1999, ApJ, 520, 592